Theoretical and Applied Fracture Mechanics 3 (1985) 185–191
North-Holland

APPLICATION OF THE STRAIN ENERGY DENSITY CRITERION TO DUCTILE FRACTURE

C.L. CHOW

Department of Mechanical Engineering, University of Hong Kong, Hong Kong

XU Jilin

Institute of Mechanics, Academia Sinica, Beijing, China

The strain energy density criterion due to Sih is used to predict fracture loads of two thin plates subjected to large elastic-plastic deformation. The prediction is achieved with a finite element analysis which is based on Hill's variational principle for incremental deformations capable of solving gross yielding problems involving arbitrary amounts of deformation. The computed results are in excellent agreement with those obtained in Sih's earlier analysis and with an experimental observation.

1. Introduction

The theory of linear elastic fracture mechanics (LEFM) propounded principally by Irwin [1] has been widely accepted by design engineers to assess structural component reliability and life expectancy. The acceptance of LEFM as a useful design tool, however, has been limited to structural materials exhibiting brittle behavior such as high strength metal alloys. In those cases, where metals undergo large plastic deformation resulting in ductile fracture, the original interpretation of fracture toughness as defined by LEFM is no longer clear. Attempts to characterize ductile fracture involving, for example, COD [2–4], J-integral [5,6], nonlinear energy theory [7], T-fracture parameter [8], etc., have been made in recent years. Apparent inconsistencies still exist in their interpretation of test results with respect to specimen geometries and loading conditions. These inconsistencies raise serious doubts as to their validity in practical engineering design application to materials stressed beyond gross yielding.

Fracture of engineering component made of yielding materials is often preceded by an extensive plastic deformation. Unlike LEFM, ductile fracture is inherently a path dependent process involving irreversible energy dissipation by yielding and fracturing of materials. More recently, Sih [9–12] proposed a strain energy density criterion for characterizing the behavior of ductile fracture capable of consistently and uniquely describing the fracture process of crack initiation, subcritical crack growth and final rupture. Sih and Madenci [11,12] illustrated the application of the criterion to predict the crack initiation and growth of a cracked plate made of mild steel undergoing large scale yielding by means of the finite element analysis. No experimental data was however available in the analysis to substantiate the validity of the computed results.

The purpose of this paper attempts to examine the validity of the strain energy density criterion when applied to ductile fracture. This is done, for the first instance, by comparing the predicted fracture load and crack increment by Sih and Madenci [11, 12] with those based on an alternative elasto-plastic algorithm. This is followed by analysing another center-cracked plate subjected to large plastic deformation and then comparing the predicted fracture load and crack increment with a set of separately measured data.

2. The strain energy density criterion

The strain energy density function dW/dV is defined as the total energy stored per unit volume of material under consideration. It may be evaluated from the true stress σ_{ij} and the true

0167-8442/85/$3.30

strain ϵ_{ij} as

$$\frac{dW}{dV} = \int \sigma_{ij} d\epsilon_{ij} \tag{1}$$

when W denotes the stored total energy, and V, the volume element of the material.

According to the strain energy density criterion [10], the fracture of a material occurs when an element ahead of a crack tip at a distance r reaches a critical value $(dW/dV)_c^*$. This value may be regarded as the material resistance to fracture and is obtained from

$$\left(\frac{dW}{dV}\right)_c^* = \left(\frac{dW}{dV}\right)_c - \left(\frac{dW}{dV}\right)_p \tag{2}$$

where $(dW/dV)_c$ is the absorbed specific energy up to the fracture which is an intrinsic material property measurable from the uniaxial tensile test as

$$\left(\frac{dW}{dV}\right)_c = \int_0^{\epsilon_u} \sigma d\epsilon. \tag{3}$$

Or, the above represents the area of a tensile diagram plotted in terms of the true stress-strain scale. The term, $(dW/dV)_p$, is the irreversible energy density at a stress state p along the stress-strain curve. Therefore, the quantity, $(dW/dV)_c^*$ depends on both the intrinsic material parameter, $(dW/dV)_c$ and the degree of plastic deformation at the stress state $(dW/dV)_p$. It is clear from its definition that the parameter, $(dW/dV)_c^*$, is not simply a material property for ductile fracture. It is however a material constant and equals to the absorbed specific energy up to the fracture for brittle fracture.

3. Finite element analysis

For cracked plate undergoing gross plastic deformation before final rupture occurs, large amounts of nonlinear geometrical and material deformation are often induced. The Eulerian finite element formulation incorporating the large deformation of isotropically hardening Prandtl–Reuss materials subjected to arbitrary stress level was adopted. The algorithm included the tangent modulus incremental plasticity and a first order self-correction process [13]. The formulation of rate equilibrium at any large deformation is given by the following form of virtual work equation [14].

$$\int_V \left[\tau_{ij}^* \delta D_{ij} - \tfrac{1}{2}\sigma_{ij}\delta\left(2D_{ik}D_{kj} - v_{k,i}v_{k,j}\right)\right] dV = \int_S \dot{f}_i \delta v_i dS + \int_V \dot{b}_i \delta v_i dV \tag{4}$$

where v is the vector of velocity components, V is the volume in the current state, and τ_{ij}^* is the Jaumann derivative of the Kirchhoff stress tensor. σ_{ij} and D_{ij} are the Cauchy true stress tensor and the strain rate tensor, respectively, and $\dot{f}$ and $\dot{b}$ are the nominal force intensity rates with respect to the current areas. The Jaumann derivative may be expressed as

$$\{\tau^*\} = [C][D] \tag{5}$$

where $[C]$ is the rate independent incremental constitutive matrix, same as the infinitesimal strain rate situation and $[D]$, the deformation rate. Let $\{\dot{\psi}\}$ be the vector of rates of nodal degrees of freedom, then

$$\{v\} = [N]\{\dot{\psi}\} \quad \text{and} \quad \{D\}[B]\{\dot{\psi}\},$$

The principle equation (4) may be used to formulate an Eulerian finite element rate equilibrium equation as

$$[K]\{\dot{\psi}\} = \{\dot{P}\}$$

where

$$\{\dot{P}\} = \int_V [N]^T \{\dot{b}\} dV + \int_S [N]^T \{\dot{f}\} dS$$

and

$$[K] = [K_{ep}] + [K_s] \tag{6}$$

for which

$$[K_{ep}] = \int_V [B]^T [C][B] dV,$$

$$[K_s] = \int_V [N_k]_{,i}^T \sigma_{ij} [N_k]_{,j} - 2[B_{ki}]^T \sigma_{ij} [B_{kj}] dV$$

In the above formulation, $[K_{ep}]$ is the same as the infinitesimal deformation formula and $[K_s]$ arises from the geometric nonlinear term.

For a thin plate under plane stress condition, i.e. $\sigma_z = \tau_{xz} = \tau_{yz} = 0$, the matrix $[K_{ep}]$ and $[K_s]$ may be expressed as given in Table 1 where S denotes the element area and t refers to the in-

Table 1
$[K_{ep}]$ and $[K_s]$

$$[K_{ep}] = \frac{Et}{4(1-\nu^2)S}\begin{bmatrix} b_r b_s + \frac{1-\nu}{2}c_r c_s & \nu b_r c_s + \frac{1-\nu}{2}c_r b_s \\ \nu c_r b_s + \frac{1-\nu}{2}b_r c_s & c_r c_s + \frac{1-\nu}{2}b_r b_s \end{bmatrix}$$
$$- \frac{t}{4S\cdot S_0}\alpha_P \begin{bmatrix} b_r b_s S_1^2 + (b_r c_s + c_r b_s)S_1 S_3 + c_r c_s S_3^2 & b_r c_s S_1 S_2 + b_r b_s S_1 S_3 + c_r c_s S_2 S_3 + c_r b_s S_3^2 \\ c_r b_s S_1 S_2 + b_r b_s S_1 S_3 + c_r c_s S_2 S_3 + b_r c_s S_3^2 & c_r c_s S_2^2 + (b_r c_s + c_r b_s)S_2 S_3 + b_r b_s S_3^2 \end{bmatrix},$$

$$[K_s] = \frac{t}{4S}\begin{bmatrix} \frac{c_s c_r}{2}(\sigma_y - \sigma_x) - b_r b_s \sigma_x & -(c_r c_s + b_r b_s)\tau_{xy} - \frac{c_r b_s}{2}(\sigma_x + \sigma_y) \\ -(b_r b_s + c_r c_s)\tau_{xy} - \frac{b_r c_s}{2}(\sigma_x + \sigma_y) & -c_r c_s \sigma_y + \frac{b_r b_s}{2}(\sigma_x - \sigma_y) \end{bmatrix}$$

stantaneous element thickness defined as $t = t_0 e^{\epsilon_z}$.

$$S_0 = \tfrac{4}{9}\bar{\sigma}^2\zeta + S_1\sigma_x' + S_2\sigma_y' + 2S_3\tau_{xy},$$

$$S_1 = \frac{\sigma_x' + \nu\sigma_y'}{1-\nu^2}E,$$

$$S_2 = \frac{E}{1-\nu^2}(\sigma_y' + \nu\sigma_x')$$

$$S_3 = \frac{E}{1+\nu}\tau_{xy}$$

where ζ is defined as the gradient of the experimentally determined true stress and plastic strain curve, or $\zeta = d\bar{\sigma}/d\bar{\epsilon}_p$, and

$$b_r = \frac{\partial N_r}{\partial x}, \qquad c_r = \frac{\partial N_r}{\partial y}$$

and

$$\alpha_p = \begin{cases} 1 & \text{for plastic loading,} \\ 0 & \text{for elastic and/or unloading.} \end{cases}$$

4. Numerical analysis and results

The finite element analysis was carried out for two thin sheets, each embedded with a central crack subjected to a uniform tensile load. Due to symmetry, only a quarter of the specimen was discretized as shown in Fig. 1. The true stress-strain curve described by a power hardening law is expressed as

$$\epsilon = \frac{\sigma}{E} + \alpha\left[\left(\frac{\sigma}{\sigma_{ys}}\right)^n - 1\right] \tag{7}$$

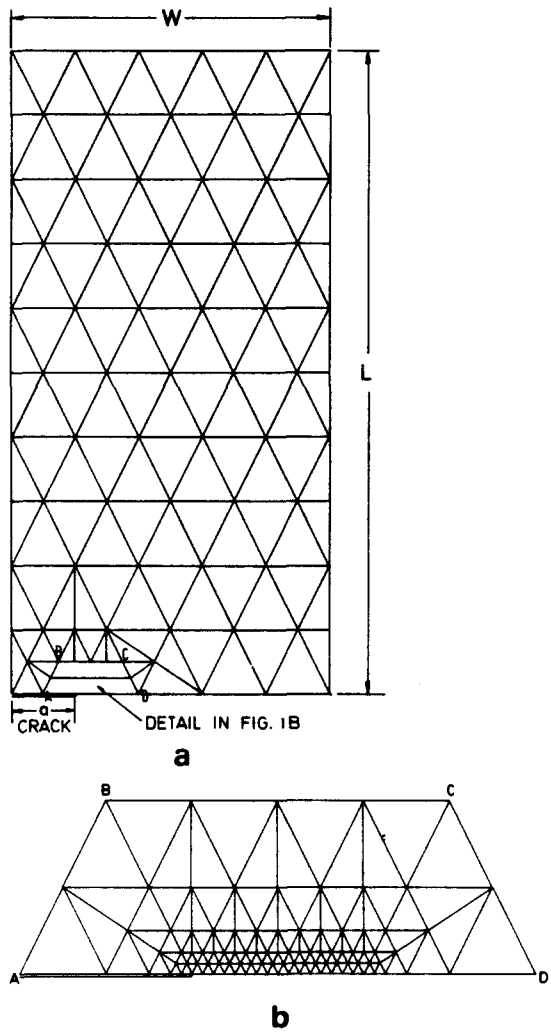

Fig. 1. (a) A quarter of center cracked plate used for finite element analysis; (b) Detailed finite element mesh of crack tip region, ABCD, shown in (a).

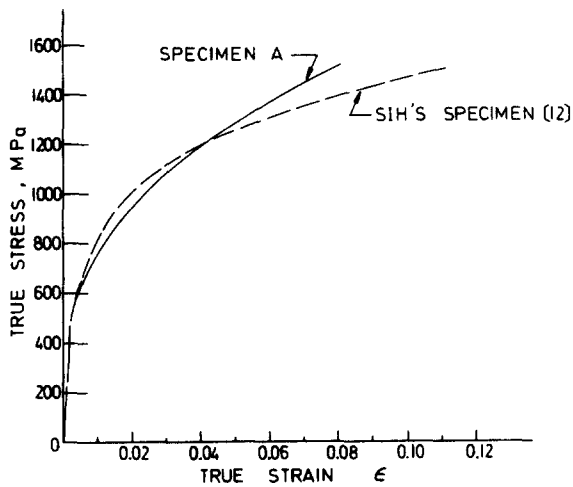

Fig. 2. True Stress – true strain curve.

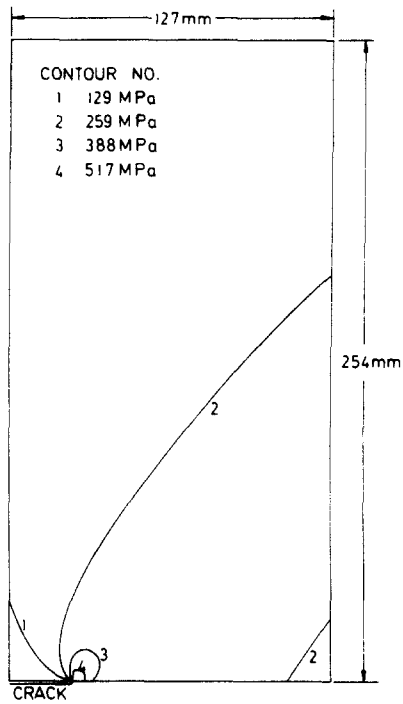

Fig. 3. Effective stress contours for applied stress of 252 MPa (Specimen A).

where E is Young's modulus, σ_{ys} is the yield stress, ϵ is the strain and σ is the stress. The coefficient α and the strain hardening exponent n are determined from the stress-strain curve measured from a thin tensile specimen under uniaxially increasing load. The multiaxial stress state computed from the finite element analysis within a cracked specimen is related to the uniaxial tensile data via the equivalent stress σ_e as

$$\sigma_e = \sqrt{\tfrac{3}{2}\sigma'_{ij}\sigma'_{ij}} \tag{8}$$

where σ'_{ij} is the stress deviator tensor. The resistance to crack growth, $(dW/dV)^*_c$, which is defined as the quantity dependent upon the degree of plastic deformation around the crack tip, was calculated using (2), (3) and (7).

4.1. Specimen A

As mentioned in the Introduction, an investigation of analysing a centre-crack plate using an alternative large elastic-plastic deformation algorithm as opposed to the one chosen by Sih and Madenci [11,12] is performed in order to provide an independent verification of the validity of the strain energy criterion. The geometry and material properties of Specimen A are particularly chosen to be similar to those described in Sih's analysis [12]. Figure 1 depicts one quarter of the specimen with half specimen height, $L = 254$ mm (10 in) and half width, $W = 127$ mm (5 in). The half crack length, a, is 25.4 mm. The yield stress and Young's modulus of the material chosen are respectively 517 MPa (75 ksi) and 207 GPa (30000 ksi). Figure 2 shows the true stress-strain curve of the material from which the material constants in (7) are evaluated as $n = 3$ and $\alpha = 0.003$. For comparison purpose, the true stress-strain curve used by Sih and Madenci [11,12] is also plotted in Fig. 2 in discontinuous line.

The rectangular plate subjected to an uniform applied load of 536 MPa (77.8 ksi) along the upper and lower boundaries was analysed and the computed equivalent stress contours and the strain energy density contours are summaried in Figs. 3 and 4 respectively. Figure 5 depicts the computed load-displacement relationship exhibiting their

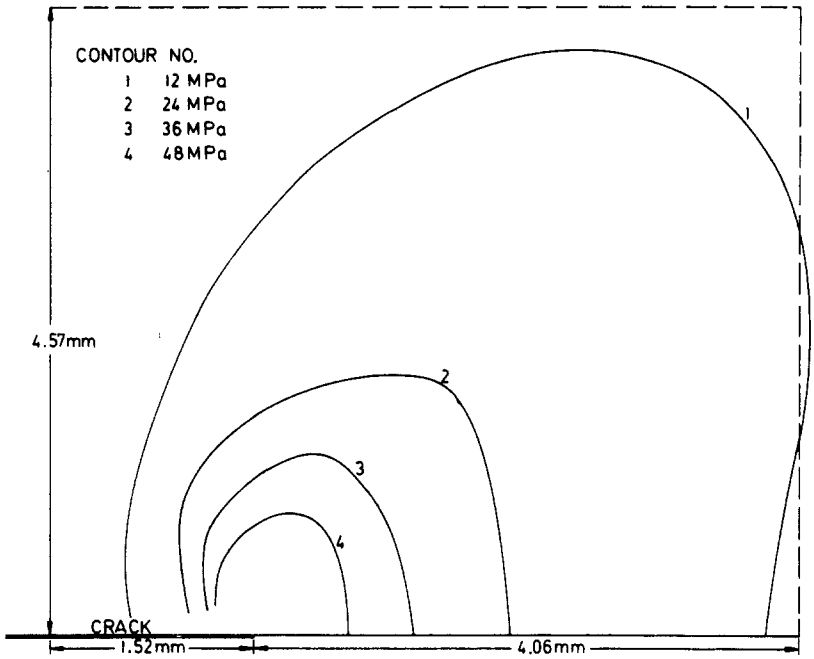

Fig. 4. Strain energy density contours for applied stress of 536 MPa (Specimen A).

smooth linear behavior up to the point where the applied load induced gross yielding of the cracked plate.

The variations of the strain energy density, (dW/dV), the crack growth resistance, $(dW/dV)_c^*$ and the equivalent stress, σ_e, along the radial distance r ahead of the crack tip at an applied load of 536 MPa are summaried in Fig. 6. It can be observed from the figure that the strain energy

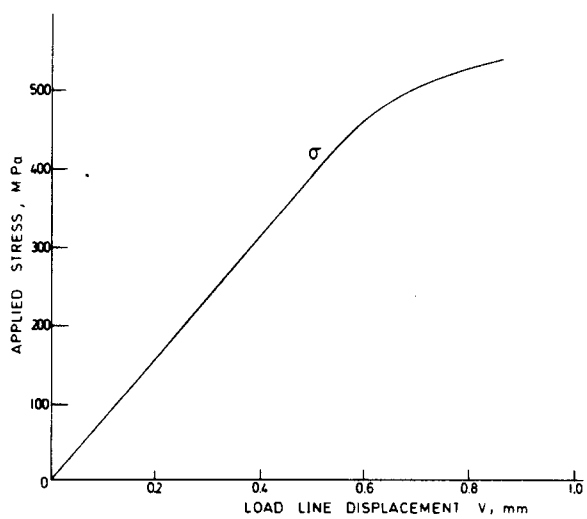

Fig. 5. Load-displacement curve (Specimen A).

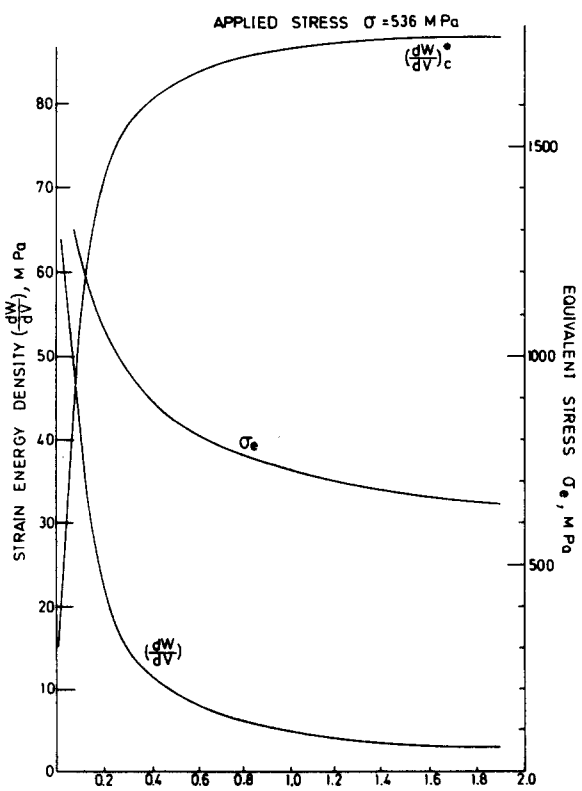

Fig. 6. Variations of strain energy density with distance r, mm.

density (dW/dV) and the equivalent stress σ_e increased rapidly with the decrease of distance r towards the crack tip. The material resistance parameter, $(dW/dV)_c^*$, on the other hand decreased with the decrease of the distance r because of the increasing degree of plasticity closer to the crack tip as illustrated in (2). According to the strain energy density criterion, crack initiation occurs when the strain energy density function, (dW/dV), is equal to the material resistance parameter $(dW/dV)_c^*$ [12]. The condition is satisfied when the element located at $r = 0.76$ mm (0.03 in) ahead of the crack tip attained the equivalent stress, σ_e, of 1310 MPa (190 ksi) shown in Fig. 6. This implies that there was an incremental crack growth of 0.76 mm when the cracked plate shown in Fig. 1 was uniformly loaded at the upper and lower boundaries to $\sigma = 536$ MPa.

As mentioned earlier, the primary purpose of analysing Specimen A is to examine the validity of the strain energy density criterion by comparing the computed results using an alternative elastic-plastic large deformation algorithm with those obtained by Sih and Madenci [12]. The results of both analyses are summarized in Table 2. Due to the use of different element sizes at the crack tip, no direct comparison can be made on the amount of crack increment induced relative to its applied load. Nevertheless, the computed crack increment and its corresponding applied load computed by the authors fall well within the range of those by Sih and Madenci as shown in Table 2.

4.2. Specimen B

An experiment was performed by Xu [13] to study stable crack growth processes of a center cracked aluminium plate subjected to uniform tensile load. This was then done to check the validity of the predicted fracture load based on an elongation criterion [13] for a thin sheet undergoing gross plastic deformation. The measured yield and ultimate strengths of the aluminium alloy LY12-CZ used were 320 MPa and 510 MPa respectively. The strain hardening exponent n was found to be 5.3 and α, 0.012. The height and width of the specimen chosen for the investigation were 180 mm and 108 mm respectively. A center crack of 11.55 mm length was embedded in the rectangular plate.

The centre cracked specimen was loaded using an universal testing machine. The specimen was fatigue-precracked and then subjected to monotonically increasing tensile load. The amount of crack extension was measured using a microscope of 80 magnification. The deformation around the crack tip was measured using laser speckle interferometry on one side of specimen surface and Moire-method on the other side.

At an applied load of 303 MPa, the computed variations of the strain energy density (dW/dV) and resistance to crack growth $(dW/dV)_c^*$ were plotted along the radial distance r from the crack tip in Fig. 7. It can be observed from the figure that the crack initiation is predicted at fracture load of 303 MPa at an increment of 0.3 mm when the condition (dW/dV) equal to $(dW/dV)_c^*$ was satisfied. These results are compared with the experimentally measured fracture load of 286 MPa as outlined in Table 3. Also shown in the table is the predicted fracture of 305 MPa due to an

Table 2
Specimen A

Analysis	Crack increment (mm)	Applied load (MPa)
Sih and Madenci [12]	0.559	491.3
	1.346	581.7
Chow and Xu	0.762	536.4

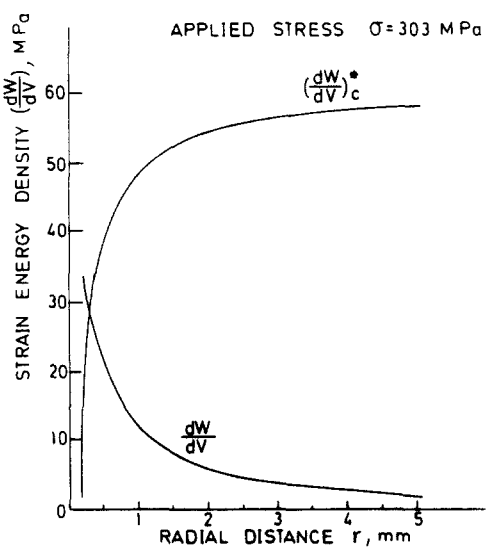

Fig. 7. Variations of strain energy density function with distance from crack tip (Specimen B).

Table 3
Specimen B

Analysis	Applied load at crack initiation (MPa)
Strain energy density criterion	303
Elongation criterion	305
Experiment	286

elongation failure criterion [13]. The elongation failure criterion postulates that crack initiation occurs when the tensile strain at the crack tip reaches the elongation of the material at failure under the uniaxial tensile loading. The predicted ductile fracture loads using the strain energy density criterion and the elongation criterion compare favorably with the measured value and may be attributed to the fact that both adopt similar ductile failure concepts.

5. Conclusions

(1) The strain energy density criterion can be used to correctly characterize the crack initiation of thin cracked plates undergoing large elastic-plastic deformation.

(2) The accuracy of predicted crack initiation loads with the strain energy density criterion is found to be excellent when the computed results using two different elastic-plastic finite element algorithms are compared with each other and with measured fracture loads.

References

[1] G.R. Irwin, "Analysis of Stresses and Strains Near the End of a Crack Traversing A Plate", *Trans. ASME, J. Appl. Mech. 24*, 361–364 (1957).

[2] A.A. Wells, "Application of Fracture Mechanics and Beyond General Yielding", *British Welding J.*, 563–570 (November 1963).

[3] D.S. Dugdale, "Yielding of Steel Sheets Containing Slits," *J. Mech. Phys. Solids 8*, 100–104 (1960).

[4] F.M. Burdekin and D.E.W. Stone, "The Crack Opening Displacement Approach to Fracture Mechanics in Yielding Materials", *J. Strain Anal. 1*, 145–153 (1966).

[5] J.R. Rice, "A Path Independent Integral and the Approximate Analysis of Strain Concentration by Notches and Cracks," *J. Appl. Mech. 35*, 379–386 (1968).

[6] J.A. Begley and J.D. Landes, "The J-integral as a Fracture Criterion", in: *Fracture Toughness*, STP *514*, American Society for Testing and Materials (1972) 1–23.

[7] H. Liebowitz and J. Eftis, "On Nonlinear Effects in Fracture Mechanics", *Engrg. Fracture Mech. 3*, 267–281 (1971).

[8] E.H. Andrews and J.I. Bhatty, "Generalized Fracture Mechanics of Ductile Steels", *Internat. J. Fracture 20*, 65–77 (1983).

[9] G.C. Sih, "A Special Theory of Crack Propagation", in: G.C. Sih, ed., *Methods of Analysis and Solutions of Crack Problems*, Noordhoff, Leyden (1973) XXI-XLV.

[10] G.C. Sih, "Experimental Fracture Mechanics: Strain Energy Density Criterion," in G.C. Sih, ed., *Experimental Evaluation of Stress Concentration and Stress Intensity Factors*, Martinus Nijhoff, The Hague (1981) XVII-LVI.

[11] G.C. Sih and E. Madenci, "Fracture Initiation under Gross Yielding: Strain Energy Density Criterion", *Engrg. Fracture Mech. 18*, 667–677 (1983).

[12] G.C. Sih and E. Madenci, "Crack Growth Resistance Characterized by the Strain Energy Density Function", *Engrg. Fracture Mech. 18*, 1159–1171 (1983).

[13] Jilin Xu, "Analysis of Stable Crack Growth for Plane Stress by Finite Element Method," *Acta Mech. Sinica 3*, 272–279 (1982).

[14] R.M. McMeeking and J.R. Rice, "Finite Element Formulations for Problems of Large Elastic-Plastic Deformation", *Internat. J. Solids and Structures 2*, 601–616 (1975).